GEOLOGICA CARPATHICA, AUGUST 2014, 65, 4, 273–284 doi: 10.2478/geoca-2014-0018

LA-ICP-MS U-Pb apatite dating of Lower Cretaceous rocks from teschenite-picrite association in the Silesian Unit (southern Poland)

KRZYSZTOF SZOPA[1], ROMAN WŁODYKA[1] and DAVID CHEW[2]

[1]Faculty of Earth Science, University of Silesia, Będzińska Str. 60, 41-200 Sosnowiec, Poland;
krzysztof.szopa@us.edu.pl; roman.wlodyka@us.edu.pl
[2]Department of Geology, Trinity College Dublin, Dublin 2, Ireland; chewd@tcd.ie

(Manuscript received February 6, 2014; accepted in revised form June 5, 2014)

Abstract: The main products of volcanic activity in the teschenite-picrite association (TPA) are shallow, sub-volcanic intrusions, which predominate over extrusive volcanic rocks. They comprise a wide range of intrusive rocks which fall into two main groups: alkaline (teschenite, picrite, syenite, lamprophyre) and subalkaline (dolerite). Previous $^{40}Ar/^{39}Ar$ and $^{40}K/^{40}Ar$ dating of these rocks in the Polish Outer Western Carpathians, performed on kaersutite, sub-silicic diopside, phlogopite/biotite as well as on whole rock samples has yielded Early Cretaceous ages. Fluorapatite crystals were dated by the U-Pb LA-ICP-MS method to obtain the age of selected magmatic rocks (teschenite, lamprophyre) from the Cieszyn igneous province. Apatite-bearing samples from Boguszowice, Puńców and Lipowa yield U-Pb ages of 103 ± 20 Ma, 119.6 ± 3.2 Ma and 126.5 ± 8.8 Ma, respectively. The weighted average age for all three samples is 117.8 ± 7.3 Ma (MSWD = 2.7). The considerably smaller dispersion in the apatite ages compared to the published amphibole and biotite ages is probably caused by the U-Pb system in apatite being less susceptible to the effects of hydrothermal alternation than the $^{40}Ar/^{39}Ar$ or $^{40}K/^{40}Ar$ system in amphibole and/or biotite. Available data suggest that volcanic activity in the Silesian Basin took place from 128 to 103 Ma with the the main magmatic phase constrained to 128–120 Ma.

Key words: geochronology, U-Pb dating, Outer Western Carpathians, Cieszyn magmatic province, apatite.

Introduction

The Early Cretaceous alkaline volcanic region, with the teschenite-picrite association (TPA) of volcanic rocks, is unique to the western part of the Outer Western Carpathians. This magmatic province (~1500 km^2) is 15–25 km wide and extends in a NE direction for over 100 km from Hranice in Moravia, Czech Republic, to Cieszyn and Bielsko-Biała in Poland (Fig. 1). Teschenite is named after the original German name for the Teschen locality that is now divided into two parts: Těšín (in the Czech Republic) and Cieszyn (in Poland). The term "teschenite" (originally teschinite) was used for the first time by Hohenegger (1861) to describe all granular rocks from the Moravo-Silesian Beskids Mountains. Tschermak (1866) distinguished melanocratic olivine-rich rocks (picrite), confining the term teschenite to olivine-free granular rocks. The studies of Smulikowski in Cieszyn (Smulikowski 1929) and the region as a whole (Smulikowski 1930) along with the work of Pacák (1926), Mahmood (1973), and Kudlásková (1987) have provided basic knowledge on the chemistry and petrography of these rocks.

The main products of volcanic activity in the TPA are shallow, sub-volcanic intrusions, which predominate over eruptive volcanic rocks. In the Moravian part of the Cieszyn magmatic province they form submarine lava flows, sills and dykes, while in the Polish sector, they chiefly comprise sill complexes and more rarely dykes with thicknesses varying from a few centimeters to 40 meters (Konior 1963; Lemberger 1971). Minor amounts of submarine volcanism in Cieszyn (Puńców and Zamarski) were described by Gucwa et al. (1971). The teschenite-picrite association contains a wide range of intrusive rocks which belong to two main groups: alkaline (teschenite, picrite, syenite, lamprophyre) and subalkaline (typically dolerite) (Fig. 2). Based on modal relationships between plagioclase and alkaline feldspars three varieties of teschenites can be distinguished: theralitic, essexitic and monzonitic (Smulikowski 1929, 1930). The nepheline syenites occur only as small irregular bodies with sharp boundaries in the upper part of the teschenite sills or as veins cross-cutting the upper or lower chilled margins. They constitute the final product of the extensive fractional crystallization in individual teschenite sills and do not form independent intrusions. Dolerites are not very common rocks within the TPA. They contain high concentrations of SiO_2; some of the dolerite samples are quartz and hyperstene normative while others are nepheline normative using a CIPW normative mineralogy calculation (Fig. 2). Monchiquite, sannaite and camptonite represent the alkaline lamprophyre group in the TPA (Smulikowski 1929, 1930). They are very common throughout the region and form sills up to 4-6 meters thick. According to Wieser (1971), contact metamorphic assemblages indicate that temperatures of 400–500 °C were reached in the aureoles (diopside-sanidine hornfels facies) of the thickest sills.

The volcanic activity was sited in a zone parallel to the axis of the Proto-Silesian Basin (Hovorka & Spišiak 1988). It was confined to isolated tensional fissures (Hovorka & Spišiak 1988) and the upwelling magma was emplaced in an extensional horst-graben system mainly as sills into uncon-

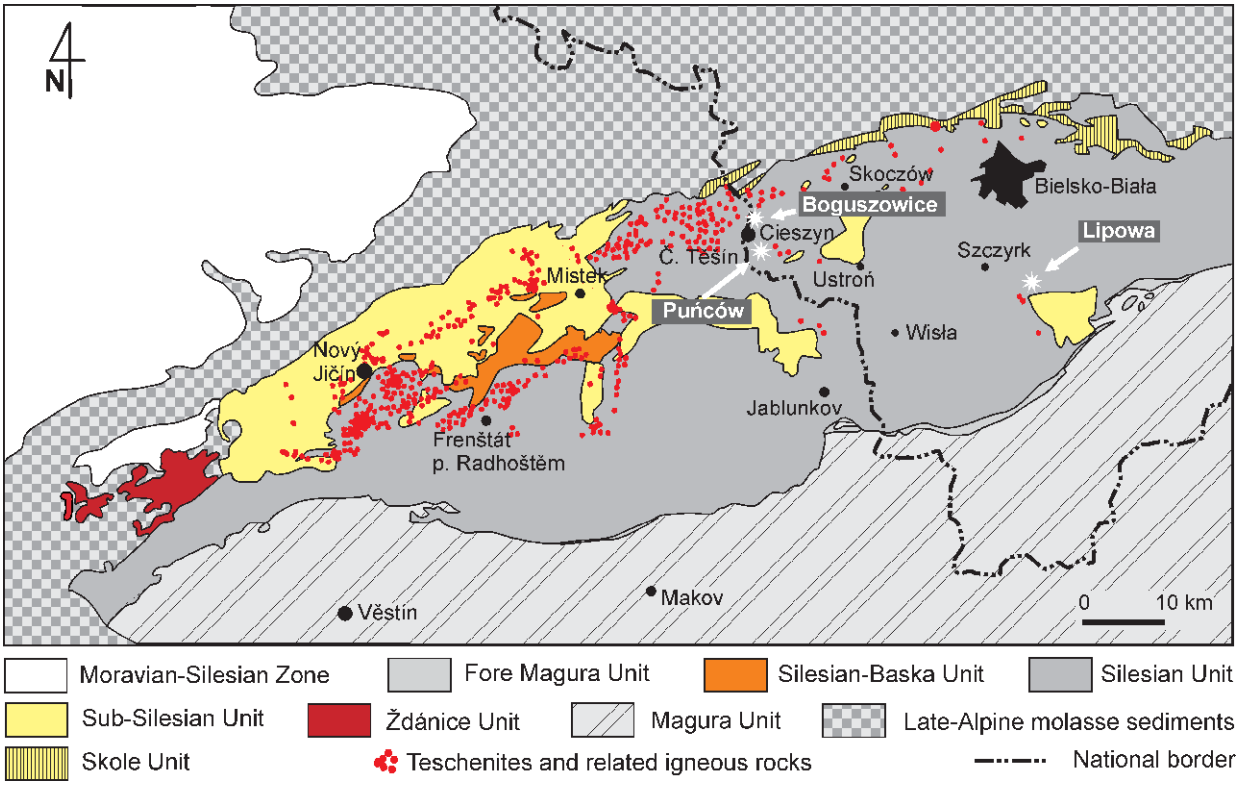

Fig. 1. Simplified geological map of the tectonic elements of the Outer Western Carpathians modified after Żytko et al. (1989). The white asterisks indicate the location of the teschenitic rocks investigated in this study. All magmatic rock localities are after Włodyka (2010).

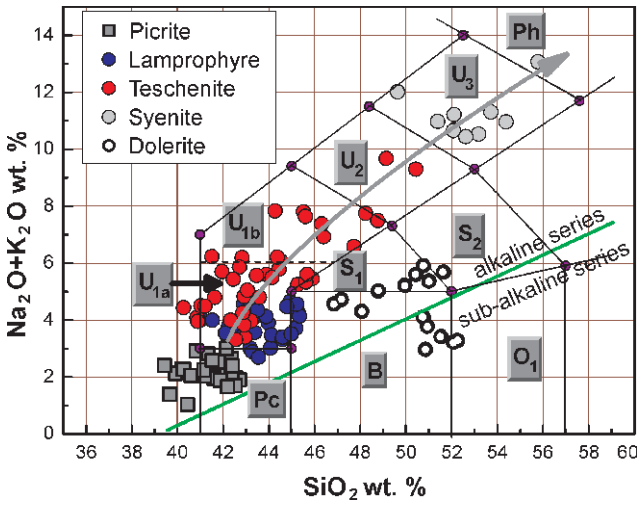

Fig. 2. Chemical classification of the TPA rocks using a TAS diagram (analyses recalculated to 100 % on an anhydrous basis). **Pc** — picrobasalt, $\mathbf{U_{1a}}$ — basanite, $\mathbf{U_{1b}}$ — tephrite, $\mathbf{U_2}$ — phonotephrite, $\mathbf{U_3}$ — tephriphonolite, **Ph** — phonolite, **B** — basalt, $\mathbf{S_1}$ — trachybasalt, $\mathbf{S_2}$ — basaltic trachyandesite, $\mathbf{O_1}$ — basaltic andesite. Filled symbols represent data from: Smulikowski 1929; Mahmood 1973; Kudlásková 1987; Dostal & Owen 1998; Włodyka 2010.

solidated Cretaceous sediments. Sometimes, on reaching the sea-floor, they flowed laterally to form local lava piles. This initial rifting phase never resulted in sea-floor spreading (Nemčok et al. 2001). The major- and trace-element patterns, and also the Nd-Sr isotopic values, indicate that the parental magma of the differentiated rocks series of the TPA was likely to have been the product of partial melting in an enriched, HIMU OIB-like upper mantle (Narębski 1990; Dostal & Owen 1998; Harangi et al. 2003; Włodyka 2010). The generation of magma is inferred to have occurred at depths of 70–80 km (Włodyka 2010). Spišiak et al. (2011) interpreted the Cretaceous alkaline volcanism in the Alpine-Carpathian-Pannonian realm as a result of partial melting of Sub-Continental Lithospheric Mantle (SCLM) on the peripheries of upwellings of asthenospheric mantle confined to slow-spreading ridges of the Alpine Tethys.

Most researchers agree on an Early Cretaceous age for the TPA, with the exception of Konior (1977) who proposed two main magmatic phases during the Cretaceous and Miocene in the Silesian Basin. $^{40}Ar/^{39}Ar$ and $^{40}K/^{40}Ar$ dating (see Table 1) on amphibole, pyroxene, phlogopite and biotite from a variety of rock types within the TPA (Lucińska-Anczkiewicz et al. 2002; Grabowski et al. 2003; Harangi et al. 2003) have yielded Early Cretaceous ages. Available geochronological and biostratigraphic data indicate that Cretaceous alkaline volcanism in the Western Carpathians (in various tectonic units of the central and external zones) started during the earliest Cretaceous (at ca. 140 Ma) and culminated during the Aptian and early Albian (from 125 to 100 Ma — Spišiak et al. 2011). In Central Europe, Lower Cretaceous alkaline rocks which exhibit close genetic and tectonomagmatic relationships to the TPA occur in the Mecsek-Alföld Igneous Province (southern Hungary, Harangi et al. 2003). K-Ar age

Table 1: Radiometric age data for the Early Cretaceous alkaline rocks of the TPA. * — $^{40}Ar/^{39}Ar$, Lucińska-Anczkiewicz et al. (2002); ** — $^{40}K/^{40}Ar$, Grabowski et al. (2003); *** — $^{40}K/^{40}Ar$, Harangi et al. (2003); **** — Apatite U-Pb data from this study.

Locality	Rock type	Analyzed fraction	Age (Ma)
Boguszowice	teschenite	amphibole	122.0±1.5* 122.4±1.1*
	monchikite	apatite	**103±20****
Międzyrzecze	picrite	flogopite	126.4±1.8**, 133.4±1.8**
Lipowa	monchikite	apatite	**126.5±8.8****
Puńców	teschenite	amphibole	111.7±1.8**, 97.0±1.8**, 99.4±1.6**, 89.9±3.5**, 96.3±3.7***
		biotite	134.9±2.0**, 137.9±2.0**
		apatite	**119.6±3.2****
	syenite	amphibole	120.4±1.3*
Rudów	teschenite	amphibole	122.2±0.9*, 112.5±1.6**
Świętoszówka	dolerite	pyroxene	122.7±4.7***
Horní Bludovice	basalt	pyroxene	122.4±6.4***
Nový Jičín	lamprophyre	amphibole	109.2±4.2***
Markov	teschenite	amphibole/biotite	109.8±4.6***
Straník	camptonite	amphibole	113.6±4.4***
Žilina	camptonite	amphibole	128.3±5.6***
Životice	lamprophyre	biotite	106.1±4.4***

data range between 130 and 110 Ma (Harangi & Árva-Sós 1993). Mesozoic teschenites are rare elsewhere although occurences have been documented in Georgia (Lebedev et al. 2009), the French Pyrenees (Azambre et al. 1992; Storetvedt et al. 1999) and Russia (Transbaikalia — Metelkin et al. 2004; Stupak et al. 2004) where volcanic activity associated with teschenite emplacement occured during the Late Cretaceous (from 86 to 110 Ma).

In this paper LA-ICP-MS U-Pb data of apatite separated from from teschenite and monchiquite rocks from the TPA are presented. Of the five main types of magmatic rocks in the TPA (Fig. 2), three (from Lipowa, Boguszowice and Puńców) yielded sufficient high quality apatite mineral separates suitable for LA-ICP-MS analysis.

Geological setting and sampling

The Outer Carpathians are sub-divided into the Subsilesian, Silesian, Fore-Magura and Magura Units (Nappes) (Oszczypko 2006) which are the structural remnants of several basins developed on the margin of the European Platform that were incorporated later into the Tertiary Carpathian accretionary wedge (Fig. 1). The Proto-Silesian Basin (Waśkowska et al. 2009) developed during Late Jurassic times as a rift and/or back-arc basin. It existed until Late Cretaceous times when it was tectoncially compartmentalized into the Silesian and Skole basins. The oldest sediments in the western part of the Proto-Silesian Basin are represented by marly shales of the Vendryně Shale Formation, previously termed the Lower Cieszyn Shales of Oxfordian-Tithonian age. This formation passes upwards into turbiditic limestones and marls of the Cieszyn Limestone Formation (Tithonian–Valanginian). The overlying Valanginian–Aptian Hradiště Formation comprises calcareous shales with intercalations of calcareous sandstones. Within this formation two members are distinguishable: a shaly facies termed the Cisownica Member (formerly termed the Upper Cieszyn Shales) and a sandstone facies termed the Piechowka Member. The Hradiště Formation is overlain by Aptian–Albian black shales of the Veřovice Formation which are in turn overlain by Albian–Early Cenomanian black shales of the Lhoty Formation.

During Late Jurassic to Aptian times the development of the Outer Carpathian basins was controlled by normal faulting and syn-rift subsidence which was associated with alkaline volcanism in the Western Carpathians. This was followed by post-rift thermal subsidence, resulting in the Albian-Cenomanian expansion of deep-water facies (Nemčok et al. 2001; Poprawa et al. 2002). The sills of alkaline rocks occur mainly in the lower part of the Hradiště Formation (the Cisownica Member) and sporadically within the underlying Cieszyn Limestone Formation and the Vendryně Shale Formation. Redeposited fragments of these rocks have been recognized in Albian sediments of the Lhoty Formation (Geroch et al. 1972). The TPA rocks encountered at Stara Wieś (Nowak 1978), Bacharowice (Gucwa & Wieser 1985) and boreholes in the Skoczów area (Konior 1959) represent detached blocks in Miocene deposits and are believed to have been derived from the Cieszyn Beds. Heavy mineral studies from the Hradiště Formation (Cisownica Member) next to the top of a theralite teschenite sill in Rudów (Szczurowska 1961) showed the presence of detrital diopside and kaersutite grains in shale. Their origin is interpreted as the result of a disaggregation of these early teschenite sills in submarine conditions. It has been assumed that the age of these submarine eruptions was contemporaneous with the deposition of the Upper Cieszyn Shales at Rudowo (Late Valanginian — Grabowski et al. 2003). The above stratigraphic data suggest the duration of the alkaline volcanism ranged from the Valanginian through to the Aptian.

Analytical techniques

Apatite crystals were separated using standard techniques, including: crushing, hydrofracturing, washing, Wilfley shaking table, Frantz magnetic separator and handpicking. The separation was undertaken at the Institute of Geological Sciences, Polish Academy of Sciences, Cracow.

The morphology and chemical homogeneity of apatite crystals were investigated using a scanning FET Philips 30 electron microscope (15 kV and 1 nA) equipped with an EDS (EDAX) detector at the Faculty of Earth Sciences, University of Silesia, Sosnowiec, Poland.

Apatite analyses (major/minor elements) were carried out in the Inter-Institution Laboratory of Microanalyses of Minerals and Synthetic Substances, Warsaw (CAMECA SX-100 electron microprobe; 1 kV, 2 nA). The apatite analyses have been calculated to the sum of 50 negative charges including 24 oxygen ions and two monovalent anions (fluorine site),

according to the ideal chemical formula of apatite: $A_{10}(BO_4)_6(X)_2$ where the A site is occupied by Ca, Fe, Mn, Mg, Th, REE, Y and Na, the B site by P (substituted by S, Si) and the X site by F, Cl and OH^- ions. The hydroxyl content was calculated by normalization assumming ideal stoichiometry (i.e. no vacancies in the X site so that $F + CI + OH^- = 2$).

Apatite U-Pb data were acquired using a Photon Machines Analyte Exite 193 nm ArF Excimer laser-ablation system coupled to a Thermo Scientific iCAP Qc at the Department of Geology Trinity College Dublin. Twenty-eight isotopes (^{31}P, ^{35}Cl, ^{43}Ca, ^{55}Mn, ^{86}Sr, ^{89}Y, ^{139}La, ^{140}Ce, ^{141}Pr, ^{146}Nd, ^{147}Sm, ^{153}Eu, ^{157}Gd, ^{159}Tb, ^{163}Dy, ^{165}Ho, ^{166}Er, ^{169}Tm, ^{172}Yb, ^{175}Lu, ^{200}Hg, ^{204}Pb, ^{206}Pb, ^{207}Pb, ^{208}Pb, ^{232}Th, ^{238}U and mass 248($^{232}Th^{16}O$) were acquired using a 50 μm laser spot, a 4 Hz laser repetition rate and a fluence of 3.31 J/cm^2. A ca. 1 cm sized crystal of Madagascar apatite which has yielded a weighted average ID-TIMS concordia age of 473.5 ± 0.7 Ma (Thomson et al. 2012; Cochrane et al. 2014) was used as the primary apatite reference material in this study. McClure Mountain syenite apatite (the rock from which the $^{40}Ar/^{39}Ar$ hornblende standard MMhb is derived) was used as a secondary standard. McClure Mountain syenite has moderate but reasonably consistent U and Th contents (~23 ppm and 71 ppm — Chew & Donelick 2012) and its thermal history, crystallization age (weighted mean $^{207}Pb/^{235}U$ age of 523.51 ± 2.09 Ma) and initial Pb isotopic composition ($^{206}Pb/^{204}Pb = 17.54 \pm 0.24$; $^{207}Pb/^{204}Pb = 15.47 \pm 0.04$) are known from high-precision TIMS analyses (Schoene & Bowring 2006). Durango apatite was also analysed in this study as a secondary standard. Durango apatite is a distinctive yellow-green fluorapatite widely used as a mineral standard in apatite fission-track and (U-Th)/He dating and apatite electron micro-probe analyses. It is found as large crystals within an open pit iron mine at Cerro de Mercado, Durango, Mexico. The apatite formed between the eruptions of two major ignimbrites which have yielded a sanidine-anorthoclase ^{40}Ar–^{39}Ar age of 31.44 ± 0.18 Ma (McDowell et al. 2005). NIST 612 standard glass was used as the apatite trace element concentration reference material.

The raw isotope data were reduced using the "VizsualAge" data reduction scheme of Petrus & Kamber (2012) within the freeware IOLITE package of Paton et al. (2011). User-defined time intervals are established for the baseline correction procedure to calculate session-wide baseline-corrected values for each isotope. The time-resolved fractionation response of individual standard analyses is then characterized using a user-specified down-hole correction model (such as an exponential curve, a linear fit or a smoothed cubic spline). The data reduction scheme then fits this appropriate session-wide "model" U-Th-Pb fractionation curve to the time-resolved standard data and the unknowns. Sample-standard bracketing is applied after the correction of down-hole fractionation to account for long-term drift in isotopic or elemental ratios by normalizing all ratios to those of the U-Pb reference standards. Common Pb in the apatite standards was corrected using the ^{207}Pb-based correction method using a modified version of the VizualAge DRS that accounts for the presence of variable common Pb in the primary standard materials (Chew et al. 2014). Over the course of two months of analyses, McClure Mountain apatite ($^{207}Pb/^{235}U$ TIMS age of 523.51 ± 1.47 Ma — Schoene & Bowring 2006) yielded a U-Pb Tera-Wasserburg concordia lower intercept age of 524.5 ± 3.7 Ma with an MSWD = 0.72. The lower intercept was anchored using a $^{207}Pb/^{206}Pb$ value of value of 0.88198 derived from an apatite ID-TIMS total U-Pb isochron (Schoene & Bowring 2006).

Results

Petrography and apatite chemistry

In the Polish part of the Outer Western Carpathians outcrops of TPA alkaline and sub-alkaline rocks are scarce. The best outcrops are found in several abandoned quarries, but even at these localities the state of preservation is often very poor due to common alteration by hydrothermal fluids and/or chemical weathering. Apatite crystals were separated from rocks from three localities (Fig. 1); two within the lower part of the Hradiště Formation (Puńców, Boguszowice) and one within the Cieszyn Limestone Formation (Lipowa).

Samples collected in Puńców come from an abandoned quarry, ca. 1.5 km north of the church in Puńców village (No. 1, N 49°43′ 49.6774″ and E 18°40′ 1.9152″) and represent the central parts of a theralite-teschenite sill. The samples dated by Lucińska-Anczkiewicz et al. (2002), Grabowski et al. (2003) and Harangi et al. (2003) come from the same location. They were probably sampled from the bottom portion of the same teschenite sill which is also visible in a small outcrop by the right inflow of the Puńcówka creek. The typical medium-grained theralite-teschenite from Puńców (Figs. 3A, 4) is formed of elongated plagioclase laths sub-ophitically intergrown with purplish-red, sector-zoned sub-silicic diopside of "fassaitic" composition. In these rocks intergrowths of clinopyroxene and amphibole (kaersutite) occur, indicating simultaneous crystallization. Sometimes the intergrowth commences along a surface corresponding to a crystal face of pyroxene. During the late-stages of melt crystallization kaersutite superseded growth of pyroxenes. We can then observe sub-silicic diopsides variably replaced by late magmatic brown kaersutite (Fig. 4). It can be attributed to a reaction between pyroxene and melt at temperatures below 1050 °C (Yagi et al. 1975). The rock also contains titanomagnetite as the dominant spinel phase which is oxidized to titanomaghemite (Harańczyk et al. 1971) during extensive sub-solidus, low-temperature alteration. The feldspars are the most altered mineral phases and are replaced mainly by a mixture of zeolites (analcime, natrolite, thomsonite, mesolite) and chlorite. Individual crystals of diopside (Fig. 3B) often have rims of mica (annite-siderophyllite). Apatite crystals sometimes form inclusions in kaersutite and diopside but occur mainly in secondary mesostasis (i.e. late stage interstitial material) after decomposed plagioclase. The apatite crystals are thin (up to 0.3 mm) and forms accicular crystals up to 2 mm.

The second sample (No. 2) comes from a small closed quarry found on the bank of the Kalembianka stream in Boguszowice Valley near Cieszyn (N 49°46′ 16.39″ and E 18°37′ 25.0095″). At this locality the central and top por-

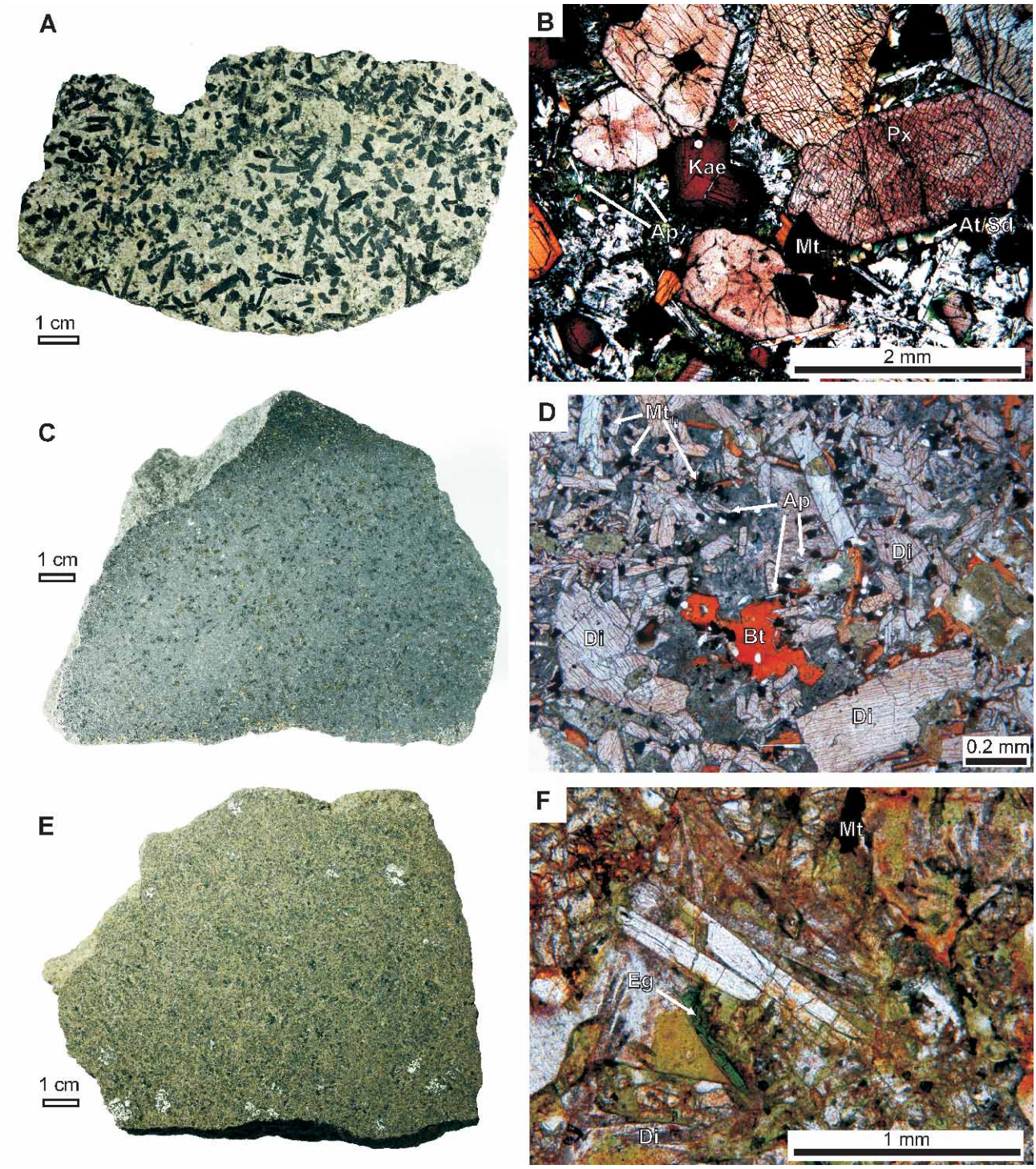

Fig. 3. Photographs of the investigated samples. Photographs **A, C** and **E** show polished rock slabs while photomicrographs **B, D** and **F** are thin sections of samples from Boguszowice, Lipowa and Puńców, respectively. **Ap** — apatite, **Bt** — biotite, **Cal** — calcite, **Chl** — chlorite, **Di** — diopside, $\mathbf{Mt_{Ti}}$ — Ti-magnetite, **Mt** — magnetite, **Kae** — kaersutite, **Eg** — aegirine, **At** — annite, **Sdf** — siderophyllite (abbreviation according to Whitney & Evans (2010)).

tions of a thin (~6 m) monchiquite sill are visible. The fine-grained central portion of the sill contains phenocrysts of sector-zoned, sub-silicic diopside and biotite (Fig. 3C). Green aegirine, locally overgrowing Al-Ti diopside is present in accessory amounts. Opaque minerals (titanomagnetite) are equally distributed throughout the rock matrix. Microcrysts of diopside, biotite, kaersutite are common in a cryptocrystalline groundmass in addition to lesser amounts of titaniferous magnetite and alkaline feldspars which are replaced by variable amounts of analcime, natrolite, calcite

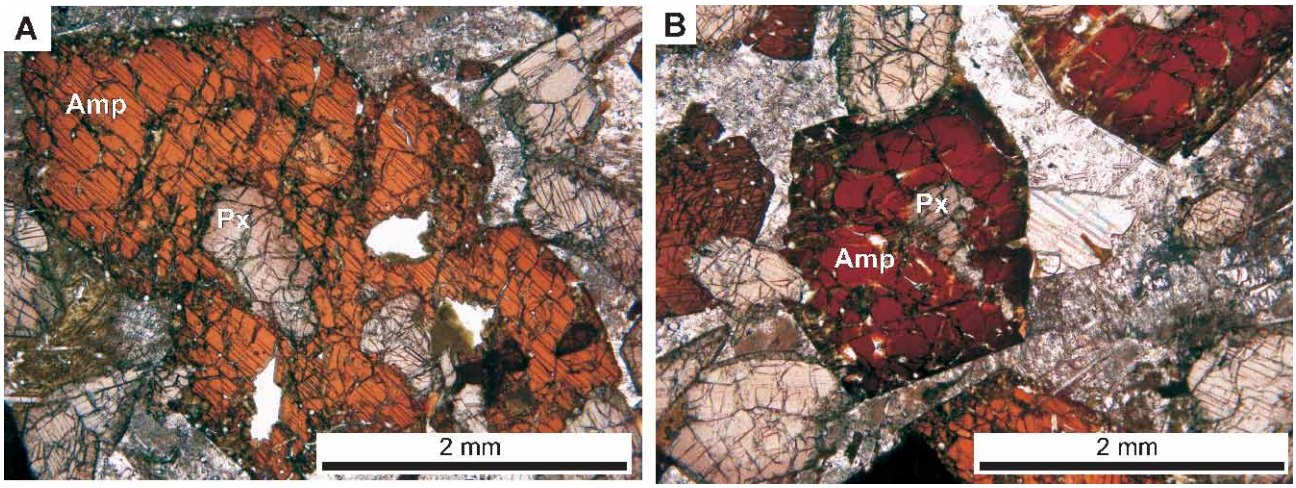

Fig. 4. An example of intergrowths of clinopyroxene and amphibole. In some cases the intergrowth commences along a surface corresponding to a crystal face of pyroxene. The crystallization of pyroxene may be followed by amphibole which then encloses small relict pyroxenes. Transmitted light, crossed polars.

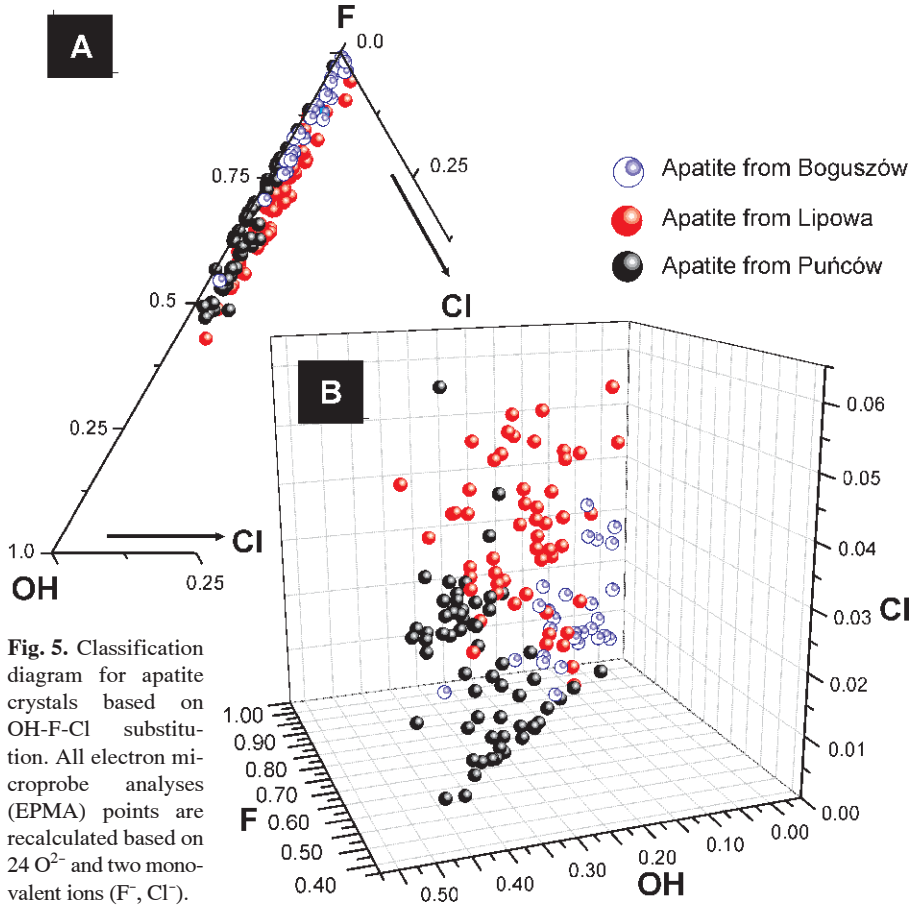

Fig. 5. Classification diagram for apatite crystals based on OH-F-Cl substitution. All electron microprobe analyses (EPMA) points are recalculated based on 24 O^{2-} and two monovalent ions (F^-, Cl^-).

and chlorite. Biotite, pyroxene and the groundmass encloses prismatic needles (up to 2.5 mm long) of apatite.

The third (No. 3) sample was collected from an abandoned quarry near Nadkościół village (N 49°40′ 51.6271″ and E 19°5′ 18.834″), to the west of Lipowa in the district of Żywiec. The apatite crystals, which take the form of long prisms up to 2–3 mm, were separated from an altered monchiquite sample (Fig. 3E,F). They occur in a groundmass of primary alkali feldspars and pyroxenes altered to an analcime-calcite-chlorite-quartz mixture. A characteristic feature of these rocks is the presence of a signifcant amount of secondary pyroxene of aegirine and aegirine-augite compositions. They form irregular rims on diopside crystals. Their secondary origin was confirmed by a fluid inclusion study by Dolníček et al. (2010).

All of the dated apatite crystals from the different magmatic rocks of the Cieszyn igneous province can be classified as fluorapatite with 1.6–3.7 wt. % F [ca. 1.4 atoms per formula unit] (Table 2; Fig. 5). The crystals range from 0.1 to 0.8 mm long and are 0.1 to 0.2 mm wide (Fig. 6); in general stubby apatite dominates over acicular varities in the studied populations. Apatite crystals in all the samples show high but variable Sr contents 2580–3218 ppm (mean value 2980 ppm), 145–184 ppm Y (mean value 171 ppm) and low Mn contents (230–540 ppm). Their chondrite (C1)-normalized REE patterns are dominated by very strong LREE fractionation (La_N/Yb_N=57.8–73.6 — Puńców, 68–77.1 — Lipowa and 67.1–72.5 — Boguszowice), minor positive Eu anomalies (1.04–1.15) for apatite from Puńców and slightly negative Eu anomalies for Lipowa (0.93–0.95) and Boguszowice (0.91–0.93) (Fig. 6; Table 3).

Table 2: Representative electron microprobe analyses of apatite (EMPA) and number of ion p.f.u. calculated on the basis of 24 O^{2-} of the investigated samples of the TPA.

	Lipowa					Boguszowice					Puńców				
	#1	#2	#3	#4	#5	#6	#7	#8	#9	#10	#11	#12	#13	#14	#15
SO_3 (wt. %)	0.48	0.24	0.22	0.53	0.33	0.51	0.06	0.07	0.05	0.00	0.00	0.03	0.00	0.01	0.00
P_2O_5	40.50	40.76	39.94	40.26	40.86	40.79	41.49	41.10	40.89	40.81	40.56	39.14	40.27	40.30	39.58
SiO_2	0.51	0.38	0.64	0.33	0.53	0.43	0.37	0.47	0.46	0.56	0.80	1.64	1.03	0.95	1.35
Y_2O_3	0.02	0.03	0.00	0.01	0.02	0.05	0.09	0.01	0.05	0.08	0.02	0.10	0.08	0.16	0.11
La_2O_3	0.21	0.21	0.16	0.07	0.14	0.22	0.10	0.09	0.17	0.19	0.25	0.54	0.40	0.47	0.53
Ce_2O_3	0.31	0.31	0.11	0.19	0.19	0.40	0.25	0.22	0.41	0.44	0.60	1.05	0.76	0.64	1.00
Pr_2O_3	0.21	0.06	0.01	0.00	0.02	0.26	0.11	0.04	0.00	0.06	0.00	0.00	0.10	0.02	0.04
Nd_2O_3	0.03	0.15	0.08	0.00	0.13	0.48	0.01	0.16	0.22	0.17	0.19	0.19	0.41	0.35	0.72
Sm_2O_3	0.08	0.05	0.01	0.05	0.00	0.00	0.08	0.11	0.17	0.14	0.01	0.11	0.00	0.11	0.00
Gd_2O_3	0.05	0.00	0.11	0.08	0.16	0.00	0.00	0.02	0.00	0.00	0.00	0.03	0.05	0.08	0.00
Dy_2O_3	0.03	0.03	0.00	0.00	0.00	0.22	0.14	0.00	0.04	0.00	0.00	0.17	0.04	0.03	0.08
Ho_2O_3	0.13	0.19	0.15	0.00	0.08	0.13	0.25	0.02	0.17	0.29	0.20	0.06	0.00	0.25	0.15
Er_2O_3	0.06	0.00	0.12	0.01	0.02	0.10	0.14	0.00	0.00	0.06	0.00	0.00	0.00	0.00	0.05
Yb_2O_3	0.04	0.00	0.00	0.21	0.06	0.10	0.00	0.00	0.04	0.04	0.08	0.01	0.04	0.00	0.05
MgO	0.04	0.08	0.11	0.05	0.24	0.07	0.12	0.18	0.01	0.04	0.00	0.01	0.01	0.02	0.01
CaO	54.38	54.27	53.52	53.99	54.74	53.81	54.99	54.72	54.18	54.03	54.23	53.24	53.86	53.88	53.17
MnO	0.04	0.01	0.02	0.00	0.00	0.06	0.03	0.00	0.00	0.06	0.06	0.02	0.06	0.06	0.05
FeO	0.12	0.13	0.13	0.16	0.16	0.10	0.14	0.20	0.04	0.10	0.05	0.10	0.24	0.10	0.14
SrO	0.28	0.60	0.28	0.36	0.28	0.46	0.25	0.25	0.39	0.39	0.37	0.38	0.37	0.39	0.39
Na_2O	0.03	0.02	0.07	0.03	0.05	0.03	0.00	0.00	0.00	0.00	0.00	0.00	0.00	0.01	0.00
F	2.37	2.33	2.61	2.90	2.41	2.27	2.96	2.28	2.88	2.94	3.60	3.48	2.97	2.90	2.80
Cl	0.23	0.24	0.38	0.32	0.20	0.35	0.10	0.18	0.14	0.11	0.06	0.06	0.13	0.08	0.18
Total	100.15	100.08	98.67	99.53	100.58	100.84	101.67	100.09	100.31	100.51	101.07	100.34	100.82	100.78	100.39
O = F.Cl	1.05	1.04	1.18	1.29	1.06	1.04	1.27	1.00	1.24	1.26	1.52	1.47	1.28	1.24	1.22
H_2O	0.59	0.59	0.40	0.29	0.58	0.60	0.35	0.64	0.36	0.34	0.04	0.07	0.32	0.36	0.37
Total	99.69	99.64	97.89	98.54	100.10	100.41	100.75	99.73	99.42	99.59	99.58	98.94	99.86	99.90	99.55
Σ_{REE+Y}	1.17	1.02	0.75	0.61	0.79	1.95	1.16	0.66	1.27	1.47	1.34	2.26	1.89	2.10	2.72
S (*apfu*)	0.06	0.03	0.03	0.07	0.04	0.07	0.01	0.01	0.01	0.00	0.00	0.00	0.00	0.00	0.00
P	5.83	5.87	5.85	5.85	5.84	5.85	5.91	5.89	5.90	5.89	5.86	5.72	5.82	5.82	5.76
Si	0.09	0.07	0.11	0.06	0.09	0.07	0.06	0.08	0.08	0.10	0.14	0.28	0.18	0.16	0.23
Y	0.00	0.00	0.00	0.00	0.00	0.00	0.01	0.00	0.00	0.01	0.00	0.01	0.01	0.01	0.01
La	0.01	0.01	0.01	0.00	0.01	0.01	0.01	0.01	0.01	0.01	0.02	0.03	0.03	0.03	0.03
Ce	0.02	0.02	0.01	0.01	0.01	0.02	0.02	0.01	0.03	0.03	0.04	0.07	0.05	0.04	0.06
Pr	0.01	0.00	0.00	0.00	0.00	0.02	0.01	0.00	0.00	0.00	0.00	0.00	0.01	0.00	0.00
Nd	0.00	0.01	0.00	0.00	0.01	0.03	0.00	0.01	0.01	0.01	0.01	0.01	0.02	0.02	0.04
Sm	0.00	0.00	0.00	0.00	0.00	0.00	0.00	0.01	0.01	0.01	0.00	0.01	0.00	0.01	0.00
Gd	0.00	0.00	0.01	0.00	0.01	0.00	0.00	0.00	0.00	0.00	0.00	0.00	0.00	0.00	0.00
Dy	0.00	0.00	0.00	0.00	0.00	0.01	0.01	0.00	0.00	0.00	0.00	0.01	0.00	0.00	0.00
Ho	0.01	0.01	0.01	0.00	0.00	0.01	0.01	0.00	0.01	0.02	0.01	0.00	0.00	0.01	0.01
Er	0.00	0.00	0.01	0.00	0.00	0.01	0.01	0.00	0.00	0.00	0.00	0.00	0.00	0.00	0.00
Yb	0.00	0.00	0.00	0.01	0.00	0.01	0.00	0.00	0.00	0.00	0.00	0.00	0.00	0.00	0.00
Mg	0.01	0.02	0.03	0.01	0.06	0.02	0.03	0.04	0.00	0.01	0.00	0.00	0.00	0.00	0.00
Ca	9.90	9.90	9.92	9.93	9.91	9.77	9.91	9.93	9.90	9.87	9.91	9.85	9.85	9.85	9.80
Mn	0.01	0.00	0.00	0.00	0.00	0.01	0.00	0.00	0.00	0.01	0.01	0.00	0.01	0.01	0.01
Fe	0.02	0.02	0.02	0.02	0.02	0.01	0.02	0.03	0.01	0.01	0.01	0.01	0.03	0.01	0.02
Sr	0.03	0.06	0.03	0.04	0.03	0.05	0.02	0.02	0.04	0.04	0.04	0.04	0.04	0.04	0.04
Na	0.01	0.01	0.02	0.01	0.01	0.01	0.00	0.00	0.00	0.00	0.00	0.00	0.00	0.00	0.00
X_{OH}	0.66	0.67	0.46	0.34	0.65	0.68	0.40	0.73	0.40	0.38	0.04	0.09	0.36	0.41	0.43
X_F	1.27	1.26	1.43	1.57	1.29	1.22	1.57	1.22	1.56	1.59	1.94	1.90	1.60	1.57	1.52
X_{Cl}	0.07	0.07	0.11	0.09	0.06	0.10	0.03	0.05	0.04	0.03	0.02	0.02	0.04	0.02	0.05
Σ_X	2.00	2.00	2.00	2.00	2.00	2.00	2.00	2.00	2.00	2.00	2.00	2.00	2.00	2.00	2.00

None of the investigated apatite crystals show any internal zonation (Fig. 7) in either optical or BSE images.

Apatite dating

Tera-Wasserburg concordia plots of the LA-ICPMS U-Pb apatite data from three magmatic samples from the TPA (a monchiquite from both Boguszowice and Lipowa and a theralite-teschenite sill from Puńców) are plotted in fig. 8 and the analytical data are listed in Table 4. All the analyses from the three samples are characterized by relatively high amounts of common Pb ($^{207}Pb/^{206}Pb$ values typically between 0.4 and 0.8). This is a function of the relatively young age of the samples and the relatively low uranium contents (3.54–6.44 ppm — Boguszowice; 2.47–5.43 ppm — Lipowa and 2.99–5.89 ppm — Puńców).

The Tera-Wasserburg concordias were anchored using initial Pb isotopic ratios calculated using the Stacey & Kramers (1975) terrestial Pb evolution model. The apatite U-Pb age was used as a starting estimate for the Stacey &

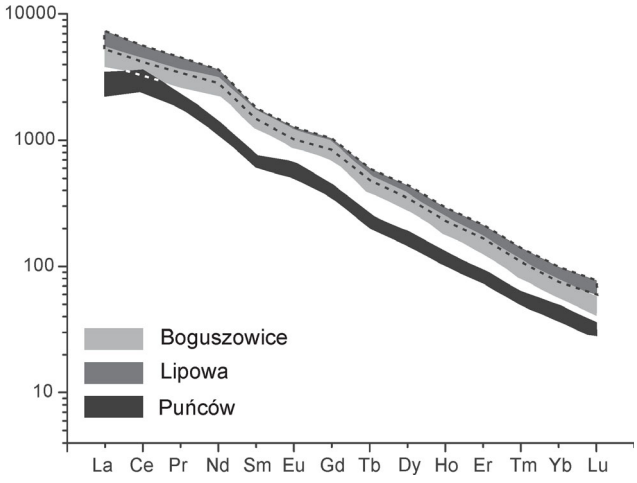

Fig. 6. Chondrite (C1)-normalized REE diagrams for apatite from the Cieszyn magma province. **Light grey area** — Boguszowice, **dark-grey** — Lipowa, **black area** — Puńców.

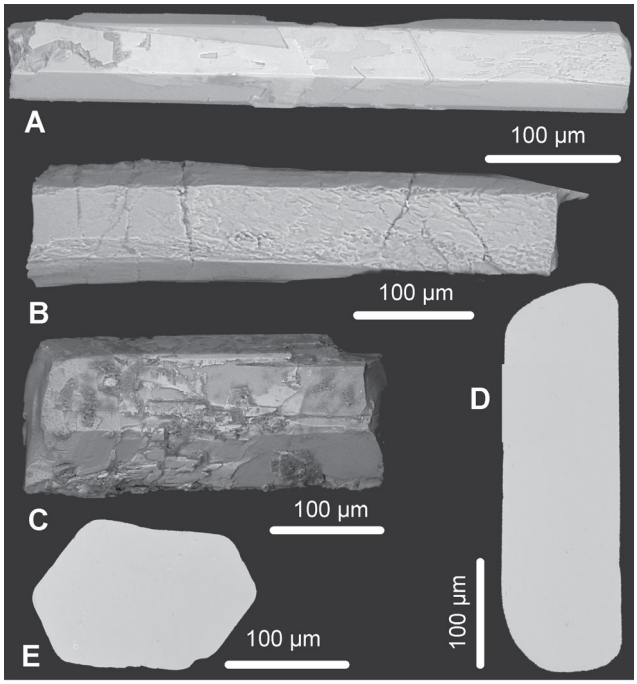

Fig. 7. BSE images of the dated apatites. **A–C** — Outer crystal surfaces, **D–E** — an examples of polished grain interiors which were used for EMP and LA-ICP-MS analysis.

Kramers (1975) model and the initial Pb isotopic composition was calculated using an iterative approach (*cf.* Chew et al. 2011). The anchored concordia lower intercept ages are 103 ± 20 Ma (MSDW = 3.5) for Boguszowice (Fig. 8A), 126.5 ± 8.8 Ma (MSDW = 1.4) for Lipowa (Fig. 8B), and 119.6 ± 3.2 Ma (MSDW = 1.4) for Puńców (Fig. 8C). Taking into account the age uncertainties, the U-Pb data cluster around 120 Ma yields a weighted average age of 117.8 ± 7.3 Ma (MSWD = 2.7). This age is consistent with the 120 Ma $^{40}Ar/^{39}Ar$ and $^{40}K/^{40}Ar$ pyroxene and amphibole

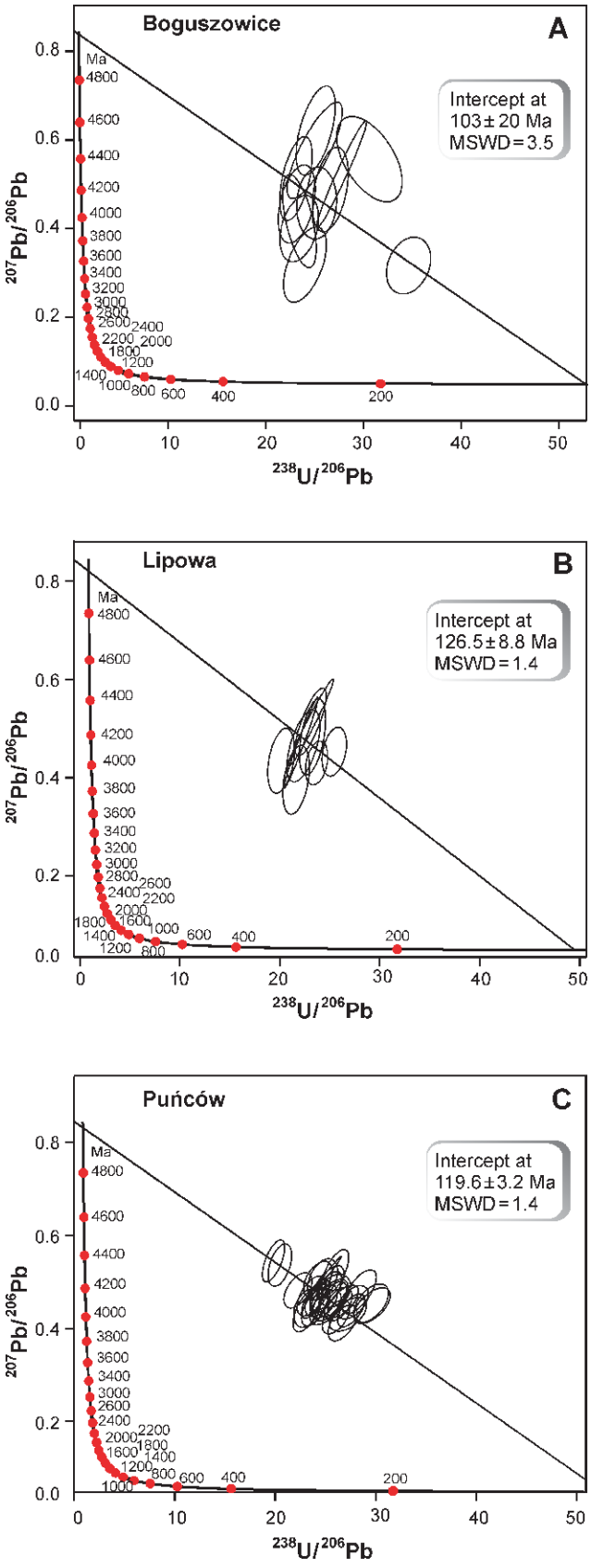

Fig. 8. Tera-Wasserburg concordia plots for LA-ICP-MS U-Pb apatite analyses from the Cieszyn igneous province (**A** — Boguszowice, **B** — Lipowa, **C** — Puńców). Data-point error ellipses are 2 σ.

Table 3: Representative LA-ICP-MS analyses of REE, Y, Mn and Sr contents in apatite crystals from this study.

Sample/ localization	Element (ppm)																		
	Mn	Sr	Y	La	Ce	Pr	Nd	Sm	Eu	Gd	Tb	Dy	Ho	Er	Tm	Yb	Lu	$(La/Yb)_n$	Eu/Eu*
Puńców	250.10	2580.53	145.92	527.02	1463.11	160.98	505.67	89.13	27.81	69.67	7.27	35.64	5.61	11.66	1.19	5.95	0.65	88.55	1.07
	231.00	2871.05	173.68	715.92	1797.30	194.29	602.38	106.35	33.49	83.64	8.85	44.36	6.72	14.17	1.46	7.36	0.84	97.31	1.08
	229.90	2708.96	176.51	683.49	1839.40	195.26	615.00	108.89	34.88	83.65	8.84	43.85	6.96	14.32	1.49	7.70	0.80	88.72	1.11
	199.90	3085.79	179.27	757.45	2036.16	208.60	652.02	111.80	37.92	88.76	9.38	45.13	7.08	14.94	1.52	7.77	0.85	97.42	1.16
	241.50	3081.20	184.91	750.16	2069.13	209.57	659.77	111.83	36.04	85.97	9.38	45.45	7.19	15.22	1.55	8.13	0.88	92.24	1.12
	231.60	2870.44	176.39	744.00	2079.68	198.08	624.04	105.50	34.41	81.71	8.90	44.66	6.65	14.28	1.51	7.58	0.82	98.19	1.13
	240.10	3218.32	177.00	752.61	2162.85	197.15	615.92	109.51	35.57	87.84	8.64	46.11	7.17	14.73	1.53	7.73	0.84	97.32	1.10
	238.10	2830.73	158.45	624.02	1665.66	172.17	568.57	98.82	31.25	77.10	7.91	41.17	6.34	13.30	1.37	7.09	0.78	88.00	1.09
	240.60	3069.73	178.22	810.46	2143.71	212.80	645.07	108.56	35.01	84.53	8.96	46.82	7.09	14.49	1.50	7.62	0.89	106.33	1.11
	245.00	2755.41	159.37	591.94	1905.00	175.82	557.99	99.05	31.84	80.05	8.32	40.84	6.28	12.83	1.41	7.09	0.75	83.50	1.09
	221.20	2840.58	166.19	637.15	1778.47	182.87	601.27	99.13	32.05	82.94	8.67	42.49	6.79	13.96	1.51	7.35	0.85	86.69	1.07
	234.80	2993.13	176.78	657.46	1720.39	179.87	621.43	107.75	33.19	83.60	9.16	44.79	6.87	14.74	1.54	7.87	0.83	83.54	1.06
Boguszowice	249.30	4440.00	372.50	1343.00	2766.00	337.60	1456.00	261.50	71.50	199.10	21.18	100.70	14.62	29.46	2.93	13.66	1.49	98.32	0.95
	229.30	4459.00	292.20	1042.00	2152.00	262.70	1147.00	205.40	55.20	155.50	16.36	78.00	11.27	22.50	2.17	10.49	1.17	99.33	0.94
	220.30	4244.00	311.90	1107.00	2286.00	281.00	1225.00	218.80	59.00	165.60	17.21	82.60	11.96	23.97	2.41	10.74	1.17	103.07	0.94
	236.50	5121.00	347.10	1248.00	2560.00	311.90	1353.00	237.60	64.70	179.30	18.79	91.00	13.56	26.58	2.62	12.29	1.36	101.55	0.95
	234.80	4601.00	319.70	1138.00	2347.00	288.20	1249.00	226.00	59.70	169.70	17.96	85.00	12.27	24.70	2.39	11.42	1.27	99.65	0.93
	231.20	4803.00	315.00	1198.00	2386.00	289.20	1265.00	221.70	60.00	168.20	17.29	83.80	11.95	24.36	2.40	10.75	1.22	111.44	0.94
	240.10	5318.00	320.60	1166.20	2390.00	290.00	1251.00	222.20	60.12	167.50	17.79	84.60	12.42	25.10	2.40	11.02	1.20	105.83	0.95
	232.40	4914.00	294.20	1046.00	2148.00	265.20	1152.00	206.00	55.35	154.70	16.14	76.80	11.42	23.00	2.35	10.17	1.11	102.85	0.94
	232.10	4946.00	286.60	1017.00	2120.00	256.10	1113.00	199.70	53.91	151.60	15.72	75.10	11.18	22.24	2.13	10.23	1.09	99.41	0.94
	258.00	4813.00	395.10	1404.00	2903.00	354.10	1538.00	275.60	74.22	208.90	21.79	102.80	15.22	31.01	3.06	14.17	1.56	99.08	0.94
Lipowa	162.00	3400.00	229.20	852.40	1758.00	207.70	887.80	149.30	39.76	113.20	12.07	58.61	8.78	18.04	1.79	8.37	1.00	101.84	0.93
	178.70	3827.00	256.20	979.00	1974.00	234.00	999.00	165.40	43.55	127.40	13.32	65.00	9.88	20.94	2.05	9.55	1.13	102.51	0.91
	181.90	4003.00	266.40	1020.00	2064.00	243.20	1030.00	170.80	45.16	131.60	13.65	67.44	10.11	21.23	2.18	10.52	1.16	96.96	0.91
	176.60	3910.00	271.60	1038.00	2090.00	246.00	1036.00	172.10	45.73	132.90	13.98	68.00	10.35	21.47	2.20	10.68	1.18	97.19	0.92
	188.00	3668.00	246.20	928.20	1901.00	223.00	955.00	160.20	42.32	122.60	12.67	61.94	9.48	19.38	1.91	9.32	1.07	99.59	0.92
	178.80	3825.00	259.60	978.00	1981.00	235.30	991.00	167.50	43.96	129.40	13.23	65.50	9.90	20.26	2.15	9.86	1.06	99.19	0.91
	189.80	3842.00	279.70	1065.00	2173.00	254.10	1074.00	179.90	46.78	135.80	14.36	69.90	10.46	22.46	2.14	10.87	1.18	97.98	0.91
	182.80	3751.00	248.00	933.00	1912.00	223.90	951.00	159.90	41.88	122.00	12.80	61.60	9.48	19.32	2.00	9.04	1.06	103.21	0.91
	181.30	3772.00	258.90	971.00	1963.00	232.20	975.00	163.70	42.97	126.10	13.09	64.10	9.59	20.34	2.07	9.56	1.16	101.57	0.91
	180.90	3845.00	285.80	1079.00	2147.00	254.50	1080.00	179.70	47.52	138.30	14.18	71.20	10.73	22.68	2.29	10.72	1.20	100.65	0.92
	175.40	3834.00	264.20	998.00	2023.00	238.80	1014.00	168.40	44.38	128.50	13.55	66.20	9.95	20.80	2.08	9.99	1.16	99.90	0.92
	182.10	4248.00	300.90	1182.00	2359.00	275.70	1158.00	190.60	50.32	143.70	15.11	75.10	11.34	24.12	2.40	11.29	1.35	104.69	0.92
LOD	0.04	2.85	0.01	0.01	0.01	0.00	0.01	0.01	0.01	0.00	0.00	0.01	0.00	0.01	0.00	0.01	0.00		

All of the calculated ratios have been done after normalizattion to chondrite-C1(Sun & McDonough 1989). **LOD** — limit of detection for concentration of analysed elements.

Table 4: Representative LA-ICP-MS U-Pb apatite data for rock samples from Boguszowice, Pańców and Lipowa.

Locality		$^{207}Pb/^{235}U$	±2σ	$^{206}Pb/^{238}U$	±2σ	ρ	$^{238}U/^{206}Pb$	±2σ	$^{207}Pb/^{206}Pb$	±2σ	ρ	$^{206}Pb/^{238}U$ age	±2σ Ma	$^{207}Pb/^{235}U$ age	±2 σ Ma	$^{207}Pb/^{206}Pb$ age	±2σ Ma	^{207}Pb corr. age	±2σ Ma	Pb tot (ppm)	Th tot (ppm)	U tot (ppm)
Lipowa	1	2.90	0.28	0.04	0.0021	0.2639	22.8833	1.10	0.48	0.05	0.33	275.73	13.3	1381.91	133.4	4171.66	393.6	128.56	16.9	11.97	67.30	84.07
	2	3.31	0.42	0.05	0.0027	–0.1308	20.0803	1.09	0.54	0.09	0.94	313.29	17.0	1483.41	188.2	4351.58	734.7	121.75	36.8	6.39	41.78	54.05
	3	3.76	0.39	0.05	0.0029	0.0006	18.9753	1.04	0.52	0.06	0.62	331.08	18.2	1584.25	164.3	4296.10	529.8	137.20	28.0	5.48	48.67	57.79
	4	3.22	0.37	0.05	0.0028	0.1276	21.4133	1.28	0.55	0.07	0.78	294.23	17.6	1461.98	168.0	4383.81	564.9	109.74	27.4	3.80	45.18	54.52
	5	2.64	0.38	0.05	0.0028	–0.1354	20.7469	1.21	0.43	0.07	0.40	303.46	17.6	1311.86	188.8	4010.48	665.3	160.50	28.8	3.67	49.10	58.00
	6	3.19	0.39	0.05	0.0033	0.1011	20.7900	1.43	0.5	0.08	0.58	302.85	20.8	1454.74	177.9	4252.95	632.9	131.05	30.2	5.07	47.84	59.20
	7	3.18	0.42	0.04	0.0024	–0.1087	22.4215	1.21	0.53	0.08	0.45	281.28	15.1	1452.31	191.8	4329.66	636.0	111.96	28.5	9.23	38.68	47.57
	8	3.45	0.47	0.05	0.0031	0.0664	20.3666	1.29	0.57	0.09	0.95	308.99	19.5	1515.87	206.5	4433.33	684.4	107.89	35.3	4.81	36.60	40.20
	9	3.54	0.47	0.05	0.0033	0.1120	19.0114	1.19	0.49	0.07	0.40	330.46	20.7	1536.20	204.0	4208.39	576.6	149.51	29.6	4.06	34.49	40.25
	10	2.85	0.27	0.04	0.0021	–0.0140	24.6305	1.27	0.5	0.05	0.34	256.55	13.3	1368.81	129.7	4252.95	438.8	110.74	17.9	4.87	67.69	86.44
Boguszowice	1	2.39	0.46	0.05	0.0042	–0.0030	22.0751	2.05	0.42	0.09	0.56	285.60	26.5	1239.61	238.6	3964.33	840.6	155.60	34.8	3.42	29.55	31.57
	2	3.32	0.49	0.05	0.0030	–0.1484	21.8341	1.43	0.59	0.10	0.59	288.68	18.9	1485.76	219.3	4478.62	754.1	94.07	36.9	2.87	35.13	35.85
	3	4.20	0.54	0.04	0.0032	0.1744	23.0947	1.71	0.72	0.10	0.59	273.26	20.2	1674.02	215.2	4771.16	662.7	43.07	35.1	2.80	36.16	40.68
	4	3.05	0.41	0.04	0.0032	0.0155	25.0627	2.01	0.67	0.10	0.18	252.21	20.2	1420.23	190.9	4667.68	696.7	55.74	32.4	2.93	36.87	43.69
	5	3.49	0.55	0.05	0.0037	0.2576	21.3675	1.69	0.56	0.09	0.44	294.85	23.3	1524.96	240.3	4417.88	705.0	105.11	34.7	2.92	31.87	40.71
	6	3.10	0.46	0.04	0.0033	0.1193	22.5225	1.67	0.55	0.08	0.28	280.05	20.8	1432.69	212.6	4367.79	673.2	106.49	30.9	3.08	33.82	35.46
	7	1.56	0.24	0.03	0.0020	0.1161	33.0033	2.18	0.4	0.06	0.32	192.43	12.7	954.47	146.8	3912.83	624.5	107.75	17.1	3.13	38.45	46.33
	8	2.72	0.51	0.05	0.0035	–0.0076	21.5517	1.63	0.46	0.09	–0.06	292.38	22.1	1333.93	250.1	4130.72	756.7	141.25	33.2	2.26	31.84	33.76
	9	2.88	0.40	0.05	0.0037	0.0847	21.5054	1.71	0.5	0.08	0.44	293.00	23.3	1376.69	191.2	4232.34	672.7	129.32	31.1	1.97	34.35	38.12
	10	3.18	0.55	0.04	0.0030	0.3107	25.0000	1.88	0.64	0.13	0.94	252.83	19.0	1452.31	251.2	4601.55	934.7	65.52	42.1	1.99	38.47	41.26
Pańców	1	2.24	0.16	0.04	0.0019	0.1243	28.0899	1.50	0.44	0.04	0.60	225.50	12.0	1193.66	85.3	4065.23	329.6	114.25	12.0	2.26	31.84	33.76
	2	2.66	0.21	0.04	0.0023	0.2949	24.3309	1.36	0.47	0.04	0.40	259.65	14.5	1317.42	104.0	4133.91	320.0	124.89	13.8	3.67	49.10	58.00
	3	2.23	0.18	0.03	0.0020	0.2040	29.4118	1.73	0.46	0.04	0.52	215.53	12.7	1190.52	96.1	4114.64	376.5	105.06	13.0	4.81	36.60	40.20
	4	2.56	0.19	0.04	0.0023	0.3213	24.8756	1.42	0.46	0.04	0.51	254.07	14.5	1289.29	95.7	4127.52	320.9	122.82	13.6	1.99	38.47	41.26
	5	2.64	0.20	0.04	0.0024	0.1546	23.5294	1.33	0.47	0.04	0.72	268.31	15.2	1311.86	99.4	4146.61	380.2	127.76	16.3	2.80	36.16	40.68
	6	2.51	0.18	0.04	0.0021	0.2417	25.3165	1.35	0.47	0.04	0.58	249.73	13.3	1274.93	91.4	4143.44	345.3	119.11	13.9	2.92	31.87	40.71
	7	2.39	0.18	0.04	0.0022	0.2946	26.2467	1.52	0.46	0.04	0.49	241.05	13.9	1239.61	93.4	4108.15	332.6	118.27	13.2	3.08	33.82	35.46
	8	2.68	0.21	0.04	0.0026	0.0658	25.3165	1.67	0.49	0.05	0.65	249.73	16.4	1322.96	103.7	4214.41	420.6	111.86	17.2	2.89	39.21	41.00
	9	2.91	0.19	0.04	0.0026	0.2958	23.9234	1.49	0.52	0.04	0.99	263.98	16.4	1384.51	90.4	4287.58	365.6	109.98	16.3	4.51	35.23	42.01
	10	2.69	0.21	0.04	0.0021	0.0922	26.1780	1.44	0.53	0.05	0.62	241.67	13.3	1325.71	103.5	4315.78	402.0	97.50	16.0	4.87	67.69	86.44

ages obtained by Lucińska-Anczkiewicz et al. (2002) and Grabowski et al. (2003) (Table 1).

Discussion

Closure temperature of apatite

Experimental determination of the diffusion parameters of Pb in apatite by high-temperature annealing experiments (Watson et al. 1985) and ion implantation with Rutherford backscattering techniques (Cherniak et al. 1991) imply closure temperatures between 450 °C and 550 °C for typical apatite grain dimensions and crustal cooling rates. These estimates are consistent with field-based studies (Chamberlain & Bowring 2000; Schoene & Bowring 2006). They are also compatible with those predicted on the basis of crystal chemistry and ionic porosity (Dahl 1997) and the empirical estimates based on U-Pb dating of large apatites from pegmatites (Krogstad & Walker 1994). Apatite is chemically stable in middle-amphibolite facies conditions (i.e. temperatures above its closure temperature). Under such conditions it is believed the U-Pb systematics of apatite are controlled predominantly by volume diffusion rather than by new growth or recrystallization (Chamberlain & Bowring 2000).

The ages of the TPA magmatic rocks range from 90 to 138 Ma (Table 4 — Lucińska-Anczkiewicz et al. 2002, 120–122 Ma; Harangi et al. 2003, 96–128 Ma; Grabowski et al. 2003, 90–138 Ma) which is longer than the tme span of magmatic activity in the Mecsek-Alföld Igneous Province in

Hungary and comparable to the range of Cretaceous alkaline volcanism documented from various tectonic units in the Western Carpathians (ca. 140 to 125–100 Ma — Spišiak et al. 2011). The very small age range between ca. 122 Ma (teschenite) and 120 Ma (nepheline syenite) emplacement documented by Lucińska-Anczkiewicz et al. (2002) is interpreted as recording the time of the solidification of teschenite sills by fractional crystallization (FC) process which is a result of crystallization of the later interstitial melts as a small irregular bodies or cross-cutting veins of nepheline syenites in the upper and lower part of the sill.

Much of the teschenite geochronological data is often somewhat contradictory as data from the same sill at an individual locality often show significant age dispersion. This is likely due to low-temperature alteration (chloritization) of the dated mafic mineral phases, and the late magmatic crystallization of amphibole. This situation is documented in Puńców where the same theralite-teschenite sill was dated by four different authors (see Table 1). The younger ages (< 100 Ma) were obtained by the K-Ar amphibole dating (Grabowski et al. 2003; Harangi et al. 2003) and Ar-Ar amphibole dating (Lucińska-Anczkiewicz et al. 2002). Petrographic studies reveal that this sill shows evidence for intensive late magmatic crystallization of amphibole (Fig. 4) which followed crystallization of pyroxene with amphibole commonly mantling pyroxene. In contrast, the oldest ages (> 130 Ma) were obtained by K-Ar dating of biotite (Puńców) and phlogopite (Międzyrzecze) (Grabowski et al. 2003).

The results obtained in this study yield similar ages (ca. 120 Ma) to those from the studies of Lucińska-Anczkiewicz et al. (2002) and Harangi et al. (2003). The apatite population is magmatic and EMP analyses and BSE observation imply no significant alternation which is common in magmatic rocks from the Cieszyn magma province. An analysis of the available robust geochronological data, including the new U-Pb apatite data from this study, suggest that volcanic activity in the Proto-Silesian Basin took place from 128 to 103 Ma and most likely peaked between 128 and 120 Ma. The U-Pb apatite dating technique has clear potential to constrain the emplacement and evolution of the Cieszyn magmatic province, as apatite is the main U-bearing phase suitable for U-Pb geochronology and the U-Pb apatite system appears unaffected by secondary alteration that has historically plagued K-Ar and ^{40}Ar-^{39}Ar dating studies on these rocks.

Conclusions

1. The weighted mean LA-ICP-MS U-Pb age for all three samples is 117.8 ± 7.3 Ma and is similar to previously published K-Ar and Ar-Ar ages.

2. The considerably smaller dispersion in the U-Pb apatite age data compared to K-Ar (whole rock) and ^{40}Ar–^{39}Ar amphibole and biotite ages is likely because the U-Pb apatite system is unaffected by alteration compared to the K-Ar and ^{40}Ar–^{39}Ar systems.

3. The probable time of volcanic activity in the Silesian Basin took place from 128 to 103 Ma and most likely peaked between 128 and 120 Ma.

4. A lack of primary magmatic zircon, monazite or xenotime makes apatite the most suitable phase for U-Pb dating of the igneous rocks from the Cieszyn magmatic province.

Acknowledgments: The authors would like to thank Jaromír Ulrych, Ján Spišiak and an anonymous reviewer who provided detailed and useful reviews of the manuscript. Piotr Dzierżanowski and Lidia Jeżak are thanked for their help during the microprobe analyses. This work was financially supported by Department of Mineralogy, Geochemistry and Petrology at Faculty of Earth Sciences, Univeristy of Silesia, Katowice.

References

Azambre B., Rossy M. & Albaréde F. 1992: Petrology of the alkaline magmatism from the Cretaceous North-Pyrenean Rift Zone (France and Spain). *Eur. J. Mineral.* 4, 813–834.

Chamberlain K.R. & Bowring A.B. 2000: Apatite-feldspar U–Pb thermochronometer: a reliable, mid-range (~450 °C), diffusion-controlled system. *Chem. Geol.* 172, 173–200.

Cherniak D.J., Lanford W.A. & Ryerson F.J. 1991: Lead diffusion in apatite and zircon using ion implantation and Rutherford backscattering techniques. *Geochim. Cosmochim. Acta* 55, 1663–1673.

Chew D.M. & Donelick R.A. 2012: Combined apatite fission track and U-Pb dating by LA-ICPMS and future trends in apatite provenance analysis. In: Sylvester P. (Ed.): Quantitative mineralogy and microanalysis of sediments and sedimentary rocks. *Mineral. Assoc. Canada*, 219–248.

Chew D.M., Sylvester. P.J. & Tubrett M.N. 2011: U-Pb and Th-Pb dating of apatite by LA-ICPMS. *Chem. Geol.* 280, 200–216.

Chew D.M., Petrus J.A. & Kamber B.S. 2014: U-Pb LA-ICPMS dating using accessory mineral standards with variable common Pb. *Chem. Geol.* 363C, 185–199.

Cochrane R., Spikings R.A., Chew D., Wotzlaw J.-F., Chiaradia M., Tyrrell S., Schaltegger U. & Van der Lelij R. 2014: High temperature (> 350 °C) thermochronology and mechanisms of Pb loss in apatite. *Geochim. Cosmochim. Acta* 127, 39–56.

Dahl P.S. 1997: A crystal-chemical basis for Pb retention and fission-track annealing systematics in U-bearing minerals, with implications for geochronology. *Earth Planet. Sci. Lett.* 150, 3–4, 277–290.

Dolníček Z., Kropáč K., Uher P. & Polách M. 2010 online: Mineralogical and geochemical evidence for multistage origin of mineral veins hosted by teschenites at Tichá, Outer Wester Carpathians, Czech Republic. *Chem. Erde.* Doi:10.1016/j.chemer.2010.03.003

Dostal J. & Owen J.V. 1998: Cretaceous alkaline lamprophyres from northeastern Czech Republic: geochemistry and petrogenesis. *Geol. Rdsch.* 87, 67–77.

Geroch S., Nowak W. & Wieser T. 1972: The occurrence of rocks of the teschenite formation on the secondary deposit in the Lower Cretaceous sediments of Beskid Mały. *Kwart. Geol.* 16, 1069–1070 (in Polish).

Grabowski J., Krzemiński L., Nescieruk P., Sszydło A., Paszkowski M., Pécskay Z. & Wójtowicz A. 2003: Geochronology of teschenitic intrusions in the Outer Western Carpathians of Poland — constraints from ^{40}K/^{40}Ar ages and biostratigraphy. *Geol. Carpathica* 54, 6, 385–393.

Gucwa I. & Wieser T. 1985: The limburgites of the Polish Carpathians. *Kwart. Geol.* 29, 3–30.

Gucwa I., Nowak W. & Wieser T. 1971: Submarine volcanism in

the Neocomian of the Western Flysch Carpathians. *Kwart. Geol*. 15, 734–735 (in Polish).

Harangi Sz. & Árva-Sós E. 1993: The Early Cretaceous volcanic rocks in the Mecsek Mts. (South Hungary). *Földt. Közl.* 123, 129–165.

Harangi Sz., Tonarini S., Vasellio O. & Manetti P. 2003: Geochemistry and petrogenesis of Early Cretaceous alkaline igneous rocks in Central Europe: implications for a long-lived EAR-type mantle component beneath Europe. *Acta Geol. Hung*. 46, 77–94.

Harańczyk C., Mahmood A. & Narębski W. 1971: Titanomaghemite in theralitic teschenite from Pastwiska near Cieszyn (Polish Carpathians). *Bull. Acad. Pol. Sci*. 19, 4, 223–231.

Hohenegger L. 1861: Die geognostischen Verhältnisse der Nordkarpaten in Schlesien und den angrenzenden Teilen von Mähren und Galizien. *Gotha*, 1–50.

Hovorka D. & Spišiak J. 1988: Mesozoic Volcanism of the Western Carpathians. *VEDA*, Bratislava, 1–263 (in Slovak, with English summary).

Konior K. 1959: The character and the age of igneous rocks intrusion of Cieszyn Silesia. *Acta Geol. Pol*. 9, 4, 445–498 (in Polish).

Konior K. 1963: Real thicknesses of igneous rocks of Cieszyn Silesia between Cieszyn and Bielsko. *Przegl. Geol*. 11, 288–290 (in Polish).

Konior K. 1977: Further comments on the age of teschenites. *Kwart. Geol.* 21, 499–513 (in Polish).

Krogstad E.J. & Walker R.J. 1994: High closure temperatures of the U-Pb system in large apatites from the Tin Mountain Pegmatite, Black Hills, South Dakota, USA. *Geochim. Cosmochim. Acta* 58, 18, 3845–3853.

Kudlásková J. 1987: Petrology and geochemistry of selected rock types of teschenite association, Outer Western Carpathians. *Geol. Carpathica* 38, 5, 545–573.

Lebedev V.A., Sakhano V.G. & Yakusev A.I. 2009: Late Cenozoic volcanic activity in Western Georgia: Evidence from new isotope geochronological data. *Dokl. Earth Sci.* 427, 819–825.

Lemberger M. 1971: Tectonic conditions of the occurrence of teschenites in the Teschen region in the light of magnetic investigations. *Pr. Geol., PAN, Komisja Nauk. Geol*., 7–108 (in Polish).

Lucińska-Anczkiewicz A., Villa I.M., Anczkiewicz R. & Ślączka A. 2002: $^{40}Ar/^{39}Ar$ dating of alkaline lamprophyres from the Polish Western Carpathians. *Geol. Carpathica* 53, 45–52.

Mahmood A. 1973: Petrology of the teschenitic rock series from the type area of Cieszyn (Teschen) in the Polish Carpathians. *Ann. Soc. Geol. Pol*. 43, 2, 153–216.

McDowell F.W., McIntosh W.C. & Farley K.A. 2005: A precise ^{40}Ar–^{39}Ar reference age for the Durango apatite (U–Th)/He and fission-track dating standard. *Chem. Geol*. 214, 249–263.

Metelkin D.V., Gordienko I.V. & Xixi Zhao 2004: Paleomagnetism of Early Cretaceous volcanic rocks from Transbaikalia: argument for mesozoic strike-slip motions in Central Asian structure. *Russ. Geol. Geophys.* 45, 1404–1417.

Narębski W. 1990: Early rift stage in the evolution of western part of the Carpathians: geochemical evidence from limburgite and teschenite rock series. *Geol. Carpathica* 41, 521–528.

Nemčok M., Nemčok J., Wojtaszek M., Ludhova L., Oszczypko N., Sercombe W.J., Cieszkowski M., Paul Z., Coward M.P. & Ślączka A. 2001: Reconstruction of Cretaceous rifts incorporated in the Outer West Carpathians wedge by balancing. *Mar. Petrol. Geol.* 18, 39–64.

Nowak W. 1978: The occurrence of the teschenite rocks in the Miocene of Stara Wieś (Karpaty Bielskie). *Kwart. Geol.* 20, 105–122 (in Polish).

Oszczypko N. 2006: Late Jurassic–Miocene evolution of the Outer Carpathian fold-and-thrust belt and its foredeep basin (Western Carpathians, Poland). *Geol. Quart*. 50, 169–194.

Pacák O. 1926: Volcanic rocks of the north foothill of Moravia Beskydy. *Česká Akad. Věd a Umění*, Praha, 1–232 (in Czech).

Petrus J.A. & Kamber B.S. 2012: Vizual age: A novel approach to laser ablation ICP-MS U-Pb geochronology data reduction. *Geostandards and Geoanalytical Research* 36, 3, 247–270.

Poprawa P., Malata T. & Oszczypko N. 2002: Tectonic evolution of the Polish part of Outer Carpathians sedimentary basins — constraints from subsidence analysis. *Przegl. Geol.* 11, 1092–1108 (in Polish).

Schoene B. & Bowring S.A. 2006: U-Pb systematics of the McClure Mountain syenite: thermochronological constraints on the age of the $^{40}Ar/^{39}Ar$ standard MMhb. *Contr. Mineral. Petrology* 151, 5, 615–630.

Smulikowski K. 1929: Materials to the knowledge of igneous rocks of Cieszyn Silesia. *Arch. Tow. Nauk. we Lwowie* III, V, 1, 1–122 (in Polish).

Smulikowski K. 1930: Les roches eruptives de la zone subbeskidique en Silésie et Moravie. *Kosmos A* 54, 3, 4, 749–850.

Spišiak J., Plašienka D., Bucová J., Mikuš T. & Uher P. 2011: Petrology and palaeotectonic setting of Cretaceous alkaline basaltic volcanism in the Pieniny Klippen Belt (Western Carpathians, Slovakia). *Geol. Quart*. 55, 27–48.

Stacey J.S. & Kramers J.D. 1975: Approximation of terrestrial lead isotope evolution by a two-stage model. *Earth Planet. Sci. Lett*. 26, 207–221.

Storetvedt K.M., Márton E., Abranches M.C. & Rother K. 1999: Alpine remagnetization and tectonic rotations in the French Pyrenees. *Geol. Rdsch*. 87, 658–674.

Stupak F.M. & Travina A.V. 2004: The age of late mesozoic volcanogenic rocks of Northern Transbaikalia (estimated by the $^{40}Ar/^{39}Ar$ method). *Russ. Geol. Geophys*. 45, 280–284.

Sun S.S. & McDonough W.F. 1989: Chemical and isotopical systematics of oceanic basalts: implications for mantle composition and processes. Magmatism in the Oceanic Basins. *Geol. Soc., Spec. Publ.* 42, 313–345.

Szczurowska J. 1961: Age of teschenites on the basis of an analysis of their heavy minerals from the Upper Teschen Shales. *Kwart. Geol*. 5, 175–179 (in Polish).

Thomson S.N., Gehrels G.E., Ruiz J. & Buchwaldt R. 2012: Routine low-damage apatite U-Pb dating using laser ablation-multicollector-ICPMS. *Geochem. Geophys. Geosyst*. 13, Q0AA21. Doi:10.1029/2011GC003928

Tschermak G. 1866: Felsarten von ungewőhnlicher Zusammensetzung in der Umgebung von Teschen und Neutitschein. *Sitz.-Ber. K. Akad. Wiss., Math.-Naturwiss. Kl*. 53, 1–5, 260–287.

Waśkowska A., Golonka J., Strzeboński P., Krobicki M., Vašíček Z. & Skupien P. 2009: Early Cretaceous deposits of the Proto-Silesian Basin in Polish-Czech Flysch Carpathians. *Geologia* 35, 39–47 (in Polish).

Watson E.B., Harrison T.M. & Ryerson F.J. 1985: Diffusion of Sm, Sr, and Pb in fluorapatite. *Geochim. Cosmochim. Acta* 49, 8, 1813–1823.

Whitney D.L. & Evans B.W. 2010: Abbreviations for names of rock-forming minerals. *Amer. Mineralogist* 95, 185–187.

Wieser T. 1971: Exo- and endocontact alterations connected with teschenites of the Polish Flysch Carpathians. *Kwart. Geol.* 15, 901–920 (in Polish).

Włodyka R. 2010: The evolution of mineral composition of the Cieszyn magma province rocks. *Wyd. Uniw. Śląskiego*, 1–232 (in Polish).

Yagi K., Hariya Y., Onuma K. & Fukushima N. 1975: Stability relation of kaersutite. *J. Fac. Sci., Hokkaido Univ., Ser 4* 16, 331–342.

Żytko K., Zając R., Gucik S., Ryłko W., Oszczypko N., Garlicka I., Nemčok J., Eliáš M., Menčik E. & Stráník Z. 1989: Map of the tectonic elements of the Western Outer Carpathians and their foreland. In: Poprawa D. & Nemčok J. (Eds.): Geological Atlas of the Western Outer Carpathians and their Foreland. *Państw. Inst. Geol*., Warszawa/*GÚDŠ*, Bratislava/*UUG*, Praha.